Cube moves for s-embeddings and α-realizations

Paul Melotti, Sanjay Ramassamy, Paul Thévenin

Cube moves for s-embeddings and α-realizations

Paul Melotti Sanjay Ramassamy Paul Thévenin

March 19, 2020

Abstract

For every $\alpha \in \mathbb{R}^*$, we introduce the class of α-embeddings as tilings of a portion of the plane by quadrilaterals such that the side-lengths of each quadrilateral $ABCD$ satisfy $AB^\alpha + CD^\alpha = AD^\alpha + BC^\alpha$. When α is 1 (resp. 2) we recover the so-called s-embeddings (resp. harmonic embeddings). We study existence and uniqueness properties of a local transformation of α-embeddings (and of more general α-realizations, where the quadrilaterals may overlap) called the cube move, which consists in flipping three quadrilaterals that meet at a vertex, while staying within the class of α-embeddings. The special case $\alpha = 1$ (resp. $\alpha = 2$) is related to the star-triangle transformation for the Ising model (resp. for resistor networks). In passing, we give a new and simpler formula for the change in coupling constants for the Ising star-triangle transformation.

1 Introduction

The star-triangle transformation was first introduced by Kennelly in the context of resistor networks [11], as a local transformation which does not change the electrical properties of the network (such as the equivalent resistance) outside of the location where the transformation is performed. It consists in replacing a vertex of degree 3 by a triangle as on Figure 1, and the conductances after the transformation are given as some rational function of the conductances before it. It follows from the classical connection between resistor networks and random walks [10] that applying this star-triangle transformation to a graph with weights on the edges also preserves the probabilistic properties of the random walk on this graph. Conversely, a triangle can be made into a star, and the terminology "star-triangle transformation" is often used to refer to both these operations.

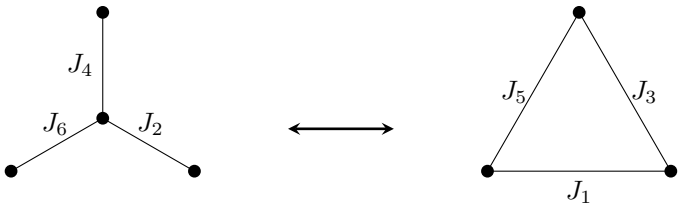

Figure 1: Star-triangle transformation.

Another probabilistic model known to possess a star-triangle transformation is the Ising model, a celebrated model of magnetization which samples a random

configuration of spins living at the vertices of a graph; this property appears in [21, 23], see also Chapter 6 of [3]. The probability distribution of this configuration depends on coupling constants attached to the edges of the graph. When these coupling constants are positive (which is called the ferromagnetic regime), one can perform a local transformation of the graph as on Figure 1 without changing the correlations of spins outside of the location where the transformation is performed [21, 23]. Note however that the formulas relating the coupling constants before and after the transformation are not the same as those for the conductances in resistor networks.

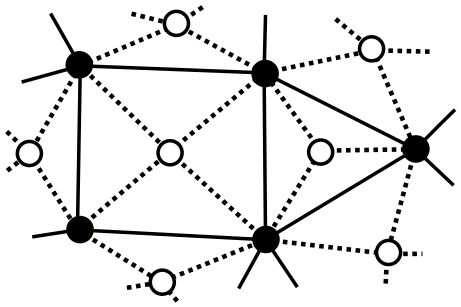

Figure 2: A piece of a planar graph G (black dots and solid lines), its dual vertices (white dots) and its diamond graph $G^\diamond$ (dotted lines).

To each of these two cases (random walk and Ising model) is associated a class of graph embeddings. More precisely, if G denotes a planar graph carrying positive edges weights (conductances for the random walk, coupling constants for the Ising model), one embeds in the plane the diamond graph $G^\diamond$, whose vertex set is composed of the vertices and dual vertices of G and whose faces are all quadrilaterals, one for each edge of G (see Figure 2). The embeddings associated to random walks (resp. the ferromagnetic Ising model) are called the Tutte embeddings or harmonic embeddings [22] (resp. s-embeddings [5]). They have the property that the faces of $G^\diamond$ are embedded as orthodiagonal quads (resp. tangential quads), that is, their diagonals are perpendicular (resp. there exists a circle tangential to the four sides). Such embeddings provide the appropriate setting to prove the convergence of observables of these stochastic processes to conformally invariant objects such as Brownian motion or SLE processes [4, 5] in the case of arbitrary planar graphs carrying generic edge weights.

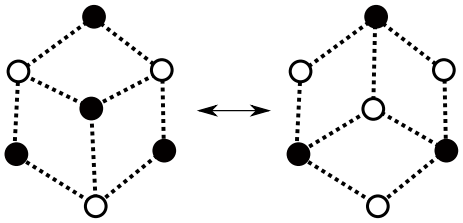

Figure 3: The transformation on $G^\diamond$ induced by the star-triangle transformation on G: a *cube move*.

The star-triangle move for random walk (resp. the Ising model) translates into a geometric local move for the harmonic embedding (resp. the s-embedding), whereby three orthodiagonal quads (resp. tangential quads) sharing a vertex as on the left-hand side picture of Figure 3 get erased and replaced by three other orthodiagonal quads (resp. tangential quads) with the same hexagonal outer boundary, as on the right-hand side picture of Figure 3. We call this geometric local move a *cube move*, phrase which was originally introduced in [14] only with a combinatorial meaning, not a geometric one.

The existence and uniqueness of the cube move for harmonic embeddings follows from a classical theorem of planar geometry called Steiner's theorem [16, 13]. In this article, we show the existence and uniqueness of the cube move for s-embeddings (see definitions in 3 and Theorem 4.1 for the exact statement).

Theorem 1.1. *For any s-embedding with the combinatorics of the graph on the left-hand side of Figure 3, erase the central black point and keep all the other points fixed. Then there exists a unique central white point that gives an s-embedding with the combinatorics of the right-hand side of Figure 3.*

Note that this is not an immediate consequence of the existence of the star-triangle transformation for the Ising model. Firstly, the star-triangle transformation might have a non-local effect on s-embeddings. Secondly, uniqueness is not clear a priori, as after removing the central black dot, the figure might be achievable as the s-embedding of some other Ising weights. We show in particular that these obstructions do not hold. In passing we prove new and simpler formulas for the transformation of coupling constants under the Ising star-triangle transformation:

Theorem 1.2. *Assume J_2, J_4, J_6 (resp. J_1, J_3, J_5) denote the coupling constants before (resp. after) the star-triangle transformation for the Ising model, as on Figure 1. For every $1 \leq i \leq 6$ let θ_i be the unique angle in $(0, \frac{\pi}{2})$ such that $J_i = \frac{1}{2} \ln\left(\frac{1+\sin\theta_i}{\cos\theta_i}\right)$. Then*

$$\forall i \in \{2,4,6\},\ \cos(\theta_i) = \frac{\sin\theta_{i+3}\cos\theta_{i+1}\cos\theta_{i+5}}{\sin\theta_{i+3} + \sin\theta_{i+1}\sin\theta_{i+5}}, \tag{1.1}$$

$$\forall i \in \{1,3,5\},\ \sin(\theta_i) = \frac{\cos\theta_{i+3}\sin\theta_{i+1}\sin\theta_{i+5}}{\cos\theta_{i+3} + \cos\theta_{i+1}\cos\theta_{i+5}}, \tag{1.2}$$

where the labels are considered modulo 6.

Formulas (1.1) and (1.2) are considerably less involved than the classical transformation procedure (which is described in Proposition 4.9).

Furthermore, we introduce a one-parameter common generalization of the harmonic embeddings and the s-embeddings, which we call α-embeddings. Given $\alpha \in \mathbb{R}^*$, we call a quadrilateral $ABCD$ drawn on the plane an *α-quad* if its side lengths satisfy $AB^\alpha + CD^\alpha = AD^\alpha + BC^\alpha$. An *$\alpha$-embedding* of a graph G is an embedding of its diamond graph $G^\diamond$ such that each face of $G^\diamond$ is drawn as an α-quad. The case $\alpha = 1$ (resp. $\alpha = 2$) corresponds to s-embeddings (resp. harmonic embeddings). We also introduce the weaker notion of α-realization of G as a map from the vertices of $G^\diamond$ to the plane such that each face of $G^\diamond$ is mapped to an α-quad, with edges possibly intersecting. We provide a definition of the above notions also in the cases where $\alpha \in \{-\infty, 0, +\infty\}$. We show that,

for $\alpha > 1$, the cube move is possible for α-realizations (but the solution may not be unique). See Theorem 3.13 for a precise statement.

Theorem 1.3. *Let $\alpha > 1$. For any α-realization with the combinatorics of the graph on the left-hand side of Figure 3, erase the central black point and keep all the other points fixed. Then there exists a central white point that gives an α-realization with the combinatorics of the right-hand side of Figure 3.*

One may wonder whether a probabilistic model can be associated to α-embeddings beyond the case where α is 1 or 2. The FK-percolation model is a common generalization of the Ising model and of spanning trees (which have the same star-triangle transformation as random walks). This model also has a star-triangle transformation, however it can be applied only when the weights satisfy some local constraint [12, 7], whereas the star-triangle transformation for the Ising model and spanning trees holds without any condition on the weights. We did not succeed in relating α-embeddings to FK-percolation for arbitrary weights that would satisfy the local constraint and do no expect such a general connection to hold true. Nevertheless there exists a subclass of weights among those satisfying the local constraint which can be associated to isoradial embeddings, that is, embeddings where the quadrilateral are rhombi. In that case, the star-triangle transformation corresponds to a cube move for rhombus tilings, which exists and is unique.

Organization of the paper

In Section 2, we define our main object of interest, α-quads, and we prove a few of their basic geometric properties. We introduce in Section 3 α-embeddings and α-realizations, before defining their cube move. We then prove that, for $\alpha > 1$, such a move is always possible. Section 4 is devoted to the specific case $\alpha = 1$, where we recall the connection with the Ising model and prove the existence and uniqueness of the cube move for properly embedded graphs. We also prove Theorem 1.2. Finally, we propose in Section 5 a general framework to study a broader class of quadrilaterals. Appendix A contains a brief introduction to Jacobi elliptic functions, which are one of our main tools in the proofs of Section 4.

2 The space of α-quads

This first section is devoted to the definition of the so-called α-quads, which are the main object of interest of this paper, and to the study of some of their properties. In what follows, we denote by $\overline{\mathbb{R}}$ the set $\mathbb{R} \cup \{-\infty, +\infty\}$ of extended real numbers.

2.1 Definitions

Let us start by defining the notion of α-quads.

Definition 2.1. A quadrilateral $ABCD$ is called an *α-quad* for $\alpha \in \mathbb{R}^*$ if

$$AB^\alpha + CD^\alpha = AD^\alpha + BC^\alpha.$$

It is called a 0-quad if

$$AB.CD = AD.BC,$$

a $+\infty$-quad if

$$\max(AB, CD) = \max(AD, BC)$$

and a $-\infty$-quad if

$$\min(AB, CD) = \min(AD, BC).$$

One can immediately notice that α-quads (for $\alpha \in \overline{\mathbb{R}}$) are simply quadrilaterals $ABCD$ such that $f_\alpha(AB, CD) = f_\alpha(AD, BC)$, where for $x, y > 0$ we set $f_\alpha(x, y) = x^\alpha + y^\alpha$ if $\alpha \in \mathbb{R}^*$, $f_0(x, y) = xy$, $f_{+\infty}(x, y) = \max(x, y)$ and $f_{-\infty}(x, y) = \min(x, y)$. Such a notation calls for a generalization from f_α to any homogeneous symmetric function f of two variables, which is the purpose of Section 5.

Of particular interest are the following three families of α-quads, which were already defined in a different context:

- 1-quads correspond to *tangential quads*, *i.e.* quads such that there is a circle tangential to their four sides (see e.g. [8]) ;
- 2-quads correspond to *orthodiagonal quads*, i.e. quads whose diagonals are perpendicular (see e.g. [9]) ;
- 0-quads are known under the name of *balanced quads* [8] and contain a well-studied class of quads, the *harmonic quads*, which are defined as cyclic 0-quads (that is, 0-quads inscribed in a circle, see [2] for details).

2.2 Properties of α-quads

This part is devoted to the study of some properties of these new families of quadrilaterals. We first provide a characterization of the quadrilaterals that arise as α-quads for some value of α:

Definition 2.2. A pair of opposite sides of a quadrilateral is called an *extremal pair* if these two sides achieve both the maximum and the minimum side-lengths.

Proposition 2.3. *A quadrilateral is an α-quad for some $\alpha \in \overline{\mathbb{R}}$ if and only if it has an extremal pair.*

Proof. Let Q be a quadrilateral whose side lengths are denoted by $\ell_1, \ell_2, \ell_3, \ell_4$ in cyclic order (starting from any of them). Assume that Q has no extremal pair. Then, without loss of generality, one may assume that ℓ_1 is the maximal length and ℓ_4 the minimal length, and they are distinct. Since (ℓ_1, ℓ_3) is not an extremal pair, ℓ_3 does not achieve the minimum, thus $\ell_3 > \ell_4$ and Q is not a $-\infty$-quad. Similarly, ℓ_2 does not achieve the maximum; thus, $\ell_2 < \ell_1$ and Q is not a $+\infty$-quad. By these inequalities, $\ell_1^\alpha + \ell_3^\alpha > \ell_2^\alpha + \ell_4^\alpha$ if $\alpha > 0$ and $\ell_1^\alpha + \ell_3^\alpha < \ell_2^\alpha + \ell_4^\alpha$ if $\alpha < 0$ (and in any of these cases Q is not an α-quad). Furthermore, $\ell_1\ell_3 > \ell_2\ell_4$ and Q is not a 0-quad. Finally, Q is not an α-quad for any $\alpha \in \overline{\mathbb{R}}$.

Conversely, suppose that Q has an extremal pair. We can assume that ℓ_1 is the maximal length, ℓ_3 the minimal length, and $\ell_2 \leq \ell_4$ (up to a possible mirror symmetry). If $\ell_2 = \ell_3$ or if $\ell_4 = \ell_1$ then Q is respectively a $-\infty$-quad or

a $+\infty$-quad. Hence, we can assume that $\ell_3 < \ell_2 \leq \ell_4 < \ell_1$. Consider now the function g on $\mathbb{R}^*$ defined as

$$g : \alpha \mapsto \frac{\ell_1^\alpha + \ell_3^\alpha - \ell_2^\alpha - \ell_4^\alpha}{\alpha}.$$

The function g can be extended to a continuous function on $\mathbb{R}$ by setting $g(0) = \ln\left(\frac{\ell_1\ell_3}{\ell_2\ell_4}\right)$. By the previous inequalities, for $\alpha \to -\infty$, $g(\alpha) \sim \frac{\ell_3^\alpha}{\alpha} < 0$ and for $\alpha \to +\infty$, $g(\alpha) \sim \frac{\ell_1^\alpha}{\alpha} > 0$. Hence, by the intermediate value theorem, there exists an $\alpha \in \mathbb{R}$ such that $g(\alpha) = 0$ and Q is an α-quad. □

In a second time, we characterize quadrilaterals that are α-quads for at least two distinct values of α.

Definition 2.4. A quadrilateral $ABCD$ is said to be a *kite* if its side lengths satisfy

$$\{AB, CD\} = \{BC, DA\}.$$

Proposition 2.5. *Let $\alpha \neq \alpha' \in \overline{\mathbb{R}}$, and let Q be a quad which is an α-quad and an α'-quad at the same time. Then Q is a kite.*

This generalizes a result of [8] which claims that a quad which is both a 0-quad and a 1-quad is a kite.

Proof. Denote by $\ell_1, \ell_2, \ell_3, \ell_4$ the side-lengths of Q in cyclic order. Assume first that neither α nor α' take the values $-\infty, \infty$ or 0. Then, up to replacing ℓ_i by $\ell_i^{\alpha'}$, one may assume that $\alpha' = 1$. Write $s = \ell_1 + \ell_3$ and $t = \ell_1^\alpha + \ell_3^\alpha$. Since Q is a 1-quad, we have $\ell_4 = s - \ell_2$. Since Q is also an α-quad, we have

$$\ell_2^\alpha + (s - \ell_2)^\alpha = t, \tag{2.1}$$

and $0 \leq \ell_2 \leq s$. The function $x \mapsto x^\alpha + (s-x)^\alpha$ is strictly monotonous on $[0, s/2]$ symmetric with respect to $x = s/2$, so that the only solutions of equation (2.1) are $\ell_2 = \ell_1$ and $\ell_2 = \ell_3$. Hence $\{\ell_1, \ell_3\} = \{\ell_2, \ell_4\}$, and Q is a kite.

Assume now that $\alpha = 0$ and α' is finite, one may again assume that $\alpha' = 1$, in which case the sums and products of each pair $\{l_1, l_3\}$ and $\{l_2, l_4\}$ are equal, and Q is again a kite. If $\alpha \in \{-\infty, \infty\}$ and α' is finite non-zero, one may again assume that $\alpha' = 1$ and the conclusion follows easily. The case when $\alpha \in \{-\infty, \infty\}$ and $\alpha' = 0$ is similar. Finally the case when $\{\alpha, \alpha'\} = \{-\infty, \infty\}$ is also easy. □

We finally provide an other characterization of α-quads, involving circumradii of the four triangles delimited by the sides and diagonals of the quad.

Proposition 2.6. *Let $ABCD$ be a quad. Let P denote the intersection point of its diagonals and suppose that P is distinct from A, B, C, D. We denote the respective circumradii of the triangles ABP, BCP, CDP and DAP by R_1, R_2, R_3 and R_4. Let $\alpha \in \overline{\mathbb{R}}$. The following are equivalent:*

1. *$ABCD$ is an α-quad ;*
2. *$f_\alpha(R_1, R_3) = f_\alpha(R_2, R_4)$.*

This result was already known for orthodiagonal quads and tangentials quads [9] and our proof below is a straightforward extension of the proof of [9, Theorem 9].

Proof. Let us denote the centers of the circumcircles of ABP, BCP, CDP, DAP by, respectively, O_1, O_2, O_3, O_4. Since AO_1B is isoceles in O_1, we have

$$AB = 2R_1 \sin \frac{\widehat{AO_1B}}{2}.$$

Since P lies on the circle centered at O_1 and going through A and B, we have that

$$\frac{\widehat{AO_1B}}{2} \in \left\{\widehat{APB}, \pi - \widehat{APB}\right\},$$

hence

$$AB = 2R_1 \sin \widehat{APB}.$$

Similarly we have

$$BC = 2R_2 \sin \widehat{BPC}$$
$$CD = 2R_3 \sin \widehat{CPD}$$
$$DA = 2R_4 \sin \widehat{DPA}$$

Observing that $\widehat{APB} = \widehat{CPD} = \pi - \widehat{BPC} = \pi - \widehat{DPA}$, we deduce that the quadruples (AB, BC, CD, DA) and (R_1, R_2, R_3, R_4) are proportional. Since f_α is homogeneous, $f_\alpha(AB, CD) = f_\alpha(BC, DA)$ if and only if $f_\alpha(R_1, R_3) = f_\alpha(R_2, R_4)$. This concludes the proof. □

Remark 2.7. Let h_1, h_2, h_3 and h_4 be the altitudes through P in the triangles ABP, BCP, CDP and DAP. For $\alpha \in \{1, 2\}$, $ABCD$ is an α-quad if and only if

$$h_1^{-\alpha} + h_3^{-\alpha} = h_2^{-\alpha} + h_4^{-\alpha},$$

see [9, Section 5]. However this does not hold for general values of α.

3 α-realizations and their cube moves

In this section, we define α-embeddings and α-realizations of graphs, and an operation on them called the cube move. First we introduce the terminology that will be useful to describe embeddings and realizations.

Definition 3.1. For $n \geq 3$, an n-tuple of distinct points $A_1, \ldots, A_n$ is said to be *proper* polygon if the line segments $[A_1A_2], [A_2A_3], \ldots, [A_{n-1}A_n], [A_nA_1]$ do not intersect except possible at their endpoints. In other words, the closed broken line $A_1, A_2, \ldots, A_n, A_1$ is a Jordan curve.

A proper polygon is said to be *positively (resp. negatively) oriented* if the points on its boundary oriented counterclockwise (*resp.* clockwise) are $A_1, A_2, \ldots, A_n$ in this order.

3.1 Embeddings and realizations

Let G be a planar graph, finite or infinite. Denote its dual graph by G^*, whose vertices are faces of G and where we connect two dual vertices if the two corresponding faces share an edge. We construct the graph $G^\diamond$ as the bipartite graph whose black (resp. white) vertices are the vertices of G (resp. G^*) and where an edge connects a black vertex to a white vertex whenever a vertex of G lies on the face associated with the corresponding vertex of G^*. In particular, all the faces of $G^\diamond$ are quadrilaterals.

Definition 3.2. Let $\alpha \in \overline{\mathbb{R}}$. An *$\alpha$-embedding* of G is an embedding of $G^\diamond$ in the plane such that every face of $G^\diamond$ is a proper α-quad.

In particular, for embedded graphs, edges cannot collapse to a point, two distinct edges cannot meet outside of their endpoints, faces have non-empty interiors and two distinct faces have disjoint interiors. This setting is the one preferred for the study of statistical mechanical models such as spanning trees and the Ising model. However, in the more general setting we consider, we need to allow drawings of graphs that are not necessarily embeddings.

Definition 3.3. Let $\alpha \in \overline{\mathbb{R}}$. An *$\alpha$-realization* of G is defined to be any map from the vertices of $G^\diamond$ to the plane such that every face of $G^\diamond$ is mapped to an α-quad.

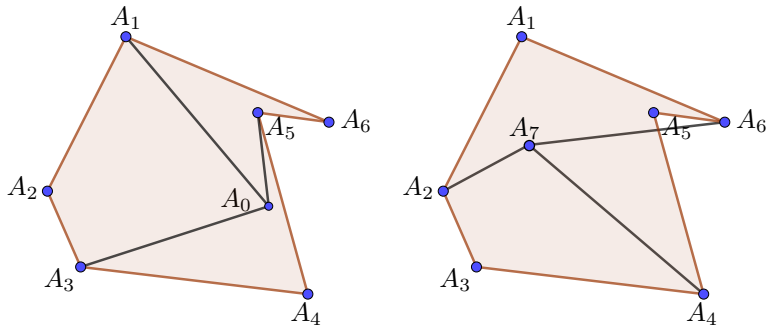

Figure 4: Here $\alpha = 4$. Left: an α-embedding of the graph on the left-hand side of Figure 5. Right: an α-realization of the graph on the right-hand side of Figure 5.

As mentioned in the introduction, there are two notable classes of examples of α-embeddings. The class of 1-embeddings of a planar graph correspond to s-embeddings defined by Chelkak in [5] (see also [19]), while the class of 2-embeddings correspond to harmonic embeddings [22, 13].

3.2 The cube move: setting

We now define the property that we want to study on α-quads, which we call the *flip property*. This property states that it is possible to perform a *cube move* like that of Figure 5 locally on the realization or embedding, while keeping the global structure unchanged.

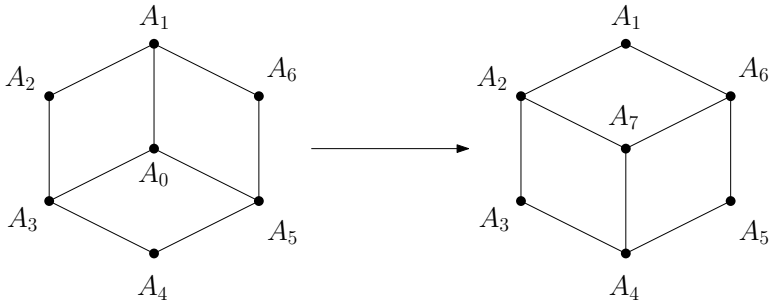

Figure 5: The combinatorics of a cube move for α-realizations and α-embeddings.

Definition 3.4. For any $\alpha \in \overline{\mathbb{R}}$, the set of α-realizations is said to satisfy the *flip property* if, for any six distinct points in the plane $A_1, A_2, \ldots, A_6$, no three of them being aligned, the following are equivalent:

- There exists a point A_0 such that $A_0, A_1, \ldots, A_6$ is an α-realization of the graph on the left-hand side of Figure 5;
- There exists a point A_7 such that $A_1, \ldots, A_7$ is an α-realization of the graph on the right-hand side of Figure 5.

The set of α-embeddings is said to satisfy the *proper flip property* if, in the equivalence of Definition 3.4, it is also required that the figures are α-embeddings, and that each of the quadrilaterals is proper, with its boundary vertices oriented in the same order as in Figure 5.

In both cases, it is said to satisfy the *unique* (proper) flip property if it satisfies the (proper) flip property and if, in addition, when the points A_0 and A_7 exist they are unique.

Our ultimate goal is to understand for which values of α these properties are verified by the set of α-realizations or α-embeddings. In this direction, we notably prove Theorem 3.13 for α-realizations with $\alpha > 1$, Theorem 4.1 for 1-embeddings, and conjecture a generalization to other values of α (see Conjecture 4.2). It is already known that the set of 2-embeddings satisfies the unique flip property; this can be proved using a Theorem of Steiner, see [16, 13].

3.3 Construction curves

In order to check the existence of the points A_0 and A_7 defined in Definition 3.4, we see them as intersection points of different curves called construction curves. Let us first define them properly.

Definition 3.5. Let A, B and C be three distinct points in the plane. For any $\alpha \in \overline{\mathbb{R}}$, the *$\alpha$-construction curve* with foci A, B going through C is the set of points M such that $ACBM$ is an α-quad.

The role of construction curves in our problem is the following. Start with a hexagon $A_1A_2A_3A_4A_5A_6$. Consider the α-construction curves $\mathcal{C}_2$ with foci

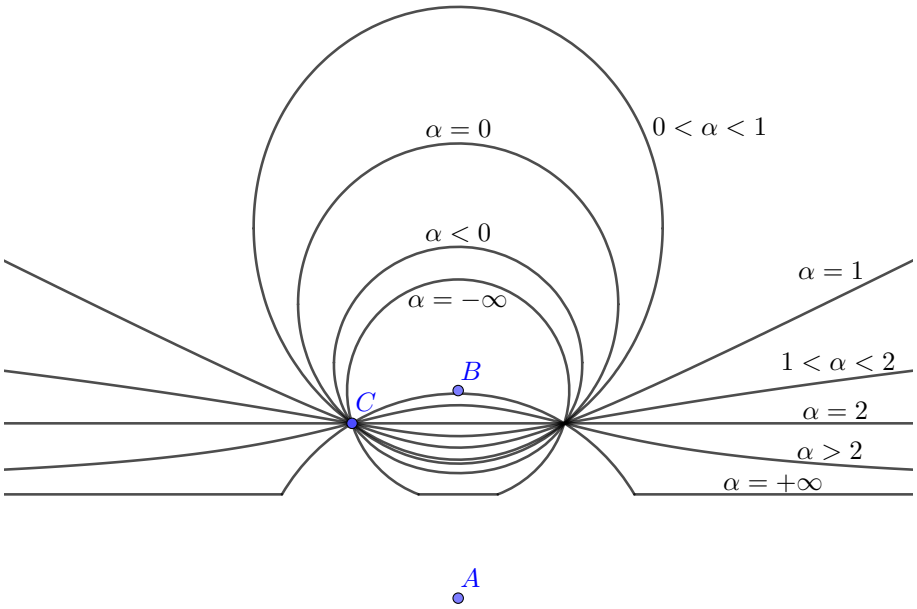

Figure 6: Construction curves with foci A and B going through C. The fact that they intersect only at C and at its symmetric with respect to (AB) is a consequence of Proposition 2.5.

A_1, A_3 going through A_2, $\mathcal{C}_4$ with foci A_3, A_5 going through A_4, and $\mathcal{C}_6$ with foci A_5, A_1 going through A_6. Then the existence of a point A_0 as on the left-hand side of Figure 5 is equivalent to the fact that $\mathcal{C}_2, \mathcal{C}_4, \mathcal{C}_6$ have a common point. A similar statement can be made for A_7. See Figure 7. We will therefore sometimes talk about these curves as construction curves of the hexagon.

In this paragraph, we aim at proving basic properties of construction curves, namely (un)boundedness, connectedness and asymptotics.

3.3.1 Special cases: $\alpha = -\infty, 0, 1, 2, +\infty$

In a few cases, the construction curves are well known. Fix A and B two points in the plane. If C is a point such that $AC = BC$, then clearly for any α the construction curve going through C is the perpendicular bisector of $[AB]$, which we denote from now on by $P(AB)$. Thus we may assume in what follows that $BC < AC$.

For any point O, we denote by $\mathcal{C}(O, C)$ the circle with center O going through C, and $\mathcal{D}(O, C)$ the closed disk enclosed by $\mathcal{C}(O, C)$.

Proposition 3.6. *Let A, and C be three points such that $BC < AB$. We denote by H the closed half-plane bounded by $P(AB)$ containing B. Then one has the following description for the α-construction curve with foci A, B going through C:*

- *For $\alpha = -\infty$, it is the union of the circular arc $\mathcal{C}(B, C) \cap H$ and the segment $P(A, B) \cap \mathcal{D}(B, C)$;*

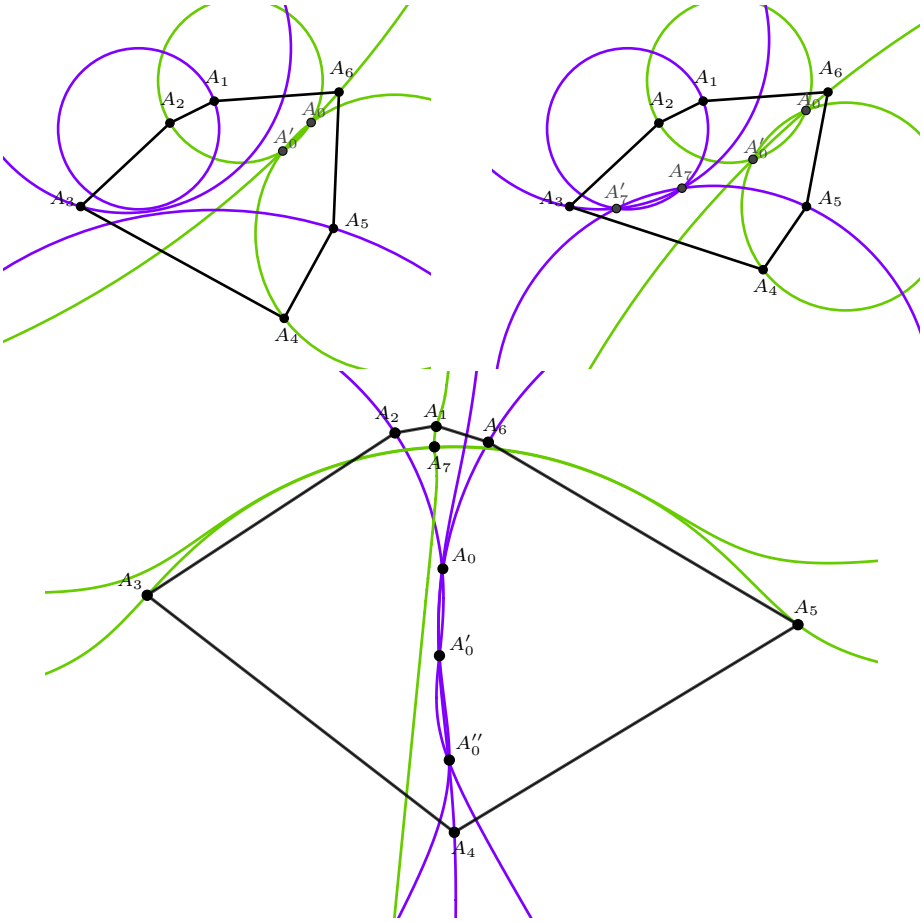

Figure 7: Examples of construction curves for some hexagons. Top left: for $\alpha = 0$, two possible points A_0 and no point A_7. Top right: for $\alpha = 0$, two points A_0 and two points A_7. Pictures with the same number of solutions as the top two pictures can be obtained for α close to 0. Bottom: for $\alpha = 10$, three points A_0 and one point A_7.

- *For $\alpha = +\infty$, it is the union of the circular arc $\mathcal{C}(A, C) \cap H$ and the two half-lines $P(A, B) \cap \mathcal{D}(A, C)^c$;*
- *For $\alpha = 0$, it is a circle going through C;*
- *For $\alpha = 1$, it is the branch closest to B of the hyperbola with foci A, B going through C;*
- *For $\alpha = 2$, it is the perpendicular to (AB) going through C.*

Proof. For $\alpha = -\infty$, the curve is $\{M \in \mathbb{R}^2 \mid \min(AM, BC) = \min(BM, AC)\}$. The explicit description follows from simple case handling, depending of the length realising the minimum. The same goes for $\alpha = +\infty$.

For $\alpha = 0$, the curve is the set of points M such that the ratio $\frac{MA}{MB}$ is fixed, which is a circle by Apollonius's circle theorem.

For $\alpha = 1$, the curve is the set of points M such that $AM - BM$ is a fixed positive number, which is a branch of hyperbola with foci A, B.

For $\alpha = 2$, as stated in Section 2, the quadrilateral $ACBM$ is a 2-quad if and only if (AB) and (CM) are perpendicular. □

3.3.2 Generic case

In the rest of this section, we restrict ourselves to $\alpha \in \mathbb{R} \setminus \{0, 1, 2\}$. Without loss of generality, we may assume that $A = (0, -1)$ and $B = (0, 1)$. Then any α-construction curve with foci A, B is characterized by a parameter $\lambda \in \mathbb{R}$, such that the curve is the set of points $\left\{M \in \mathbb{R}^2 \mid MA^\alpha - MB^\alpha = \lambda\right\}$. Hence, it is a level set of the function $F_\alpha : M \mapsto MA^\alpha - MB^\alpha$, or

$$F_\alpha(x, y) = \left(x^2 + (y+1)^2\right)^{\alpha/2} - \left(x^2 + (y-1)^2\right)^{\alpha/2}.$$

Wenote this curve by $C(\alpha, \lambda) := F^{-1}(\{\lambda\})$. Remark that when $\lambda = 0$ the curve $C(\alpha, 0)$ is $P(AB)$, which in that case is the horizontal axis. Moreover, changing λ into $-\lambda$ has the effect of reflecting the curve across $P(AB)$. Finally, note that the curve may be empty for some values of α and λ.

The following result is immediate:

Lemma 3.7. *Let M be a point distinct from A, B. Let M' be the image of M by the reflection across (AB), and M'' the image of M by the reflection across $P(AB)$. Then one has $F_\alpha(M) = F_\alpha(M') = -F_\alpha(M'')$. In particular, F_α is the zero function on $P(AB)$. Moreover F_α has a constant sign on each half-plane bounded by $P(AB)$.*

Corollary 3.8. *For $\alpha \in \mathbb{R}^*$ and $\lambda > 0$, $C(\alpha, \lambda)$ is symmetric with respect to the axis (AB) and remains on one side of $P(AB)$ (namely, the side containing B if $\alpha > 0$ and the side containing A if $\alpha < 0$).*

In order to understand the level sets of the function F_α, let us study its profile. As a result of the symmetries of Lemma 3.7, it is sufficient to do so in the quadrant $(\mathbb{R}_+)^2$.

Lemma 3.9. *For any $M = (x_M, y_M) \in (\mathbb{R}_+)^2$,*

(i) if $\alpha < 0$:

- *F_α is C^∞ on $\mathbb{R}^2 \setminus \{A, B\}$.*
- *$\lim_{M \to B} F_\alpha(M) = -\infty$ and $\lim_{x_M^2 + y_M^2 \to \infty} F_\alpha(M) = 0$.*
- *if $y_M > 0$ and $M \neq B$, then $F_\alpha(M) < 0$.*
- *if $x_M > 0$ and $y_M > 0$, $\frac{\partial F_\alpha}{\partial x}(M) > 0$.*
- *if $x_M = 0$: if $y_M < 1$, $\frac{\partial F_\alpha}{\partial y}(M) < 0$; if $y_M > 1$, $\frac{\partial F_\alpha}{\partial y}(M) > 0$.*

(ii) if $0 < \alpha < 1$:

- *F_α is continuous on $\mathbb{R}^2$, and C^∞ on $\mathbb{R}^2 \setminus \{A, B\}$.*
- *$\lim_{x_M^2 + y_M^2 \to \infty} F_\alpha(M) = 0$.*
- *if $y_M > 0$, $F_\alpha(M) > 0$.*

– *if* $x_M > 0$ *and* $y_M > 0$, $\frac{\partial F_\alpha}{\partial x}(M) < 0$.
– *if* $x_M = 0$*: if* $y_M < 1$, $\frac{\partial F_\alpha}{\partial y}(M) > 0$*; if* $y_M > 1$, $\frac{\partial F_\alpha}{\partial y}(M) < 0$.

(iii) if $\alpha > 1$, *with* $\alpha \neq 2$*:*

– F_α *is* C^1 *on* $\mathbb{R}^2$, *and* C^∞ *on* $\mathbb{R}^2 \setminus \{A, B\}$.
– *for any fixed* $x_M \geq 0$, $\lim_{y_M \to \infty} F_\alpha(M) = +\infty$.
– *for* $y_M > 0$, $F_\alpha(M) > 0$.
– *if* $x_M > 0$ *and* $y_M > 0$, *for* $\alpha < 2$, $\frac{\partial F_\alpha}{\partial x}(M) < 0$ *and for* $\alpha > 2$, $\frac{\partial F_\alpha}{\partial x}(M) > 0$.
– *if any* $x_M, y_M \geq 0$, $\frac{\partial F_\alpha}{\partial y}(M) > 0$.

Proof. First, all claims on regularity of F_α are clear. Furthermore, the sign of this function on the quadrant $(\mathbb{R}_+)^2$ is apparent as well, since $MA \geq MB$ with equality only if $x_M = 0$.

Let us now deal with the asymptotic behaviour of F_α. For $\alpha > 0$, MB^α goes to $+\infty$ as $M \to B$ and therefore $\lim F_\alpha = -\infty$. On the other hand, for any $\alpha < 1$, notice that by the mean value theorem, for any M there exists a $u \in [MA, MB]$ such that

$$F_\alpha(M) = (MA - MB)\, \alpha u^{\alpha-1} \leq \alpha AB.MB^{\alpha-1},$$

where we used the triangular inequality. This goes to 0 as MB grows. In the case $\alpha > 1$, let x_M be fixed. For any large enough y_M, by the mean value theorem, there is a $u \in [y_M - 1, y_M + 1]$ such that

$$F_\alpha(M) = u\alpha \left(x^2 + u^2\right)^{\alpha/2-1}.$$

For large y_M, this is equivalent to $\alpha y_M^{\alpha-1}$ and so tends to $+\infty$.

We finally consider the partial derivatives of F_α. For any $M \in (\mathbb{R}_+^*)^2$, one can compute:

$$\frac{\partial F_\alpha}{\partial x}(M) = \alpha x_M \left(MA^{\alpha-2} - MB^{\alpha-2}\right)$$

and its sign is apparent. Regarding the second partial derivative of F_α, we compute:

$$\frac{\partial F_\alpha}{\partial y}(M) = \alpha(y_M+1)\left(x_M^2 + (y_M+1)^2\right)^{\alpha/2-1} - \alpha(y_M-1)\left(x_M^2 + (y_M-1)^2\right)^{\alpha/2-1}. \tag{3.1}$$

Let us investigate it in the case $\alpha < 1$. When $x_M = 0$ and $y_M \neq 1$, this reduces to

$$\alpha(\operatorname{sgn}(y_M+1)|y_M+1|^{\alpha-1} - \operatorname{sgn}(y_M-1)|y_M-1|^{\alpha-1}).$$

A study of the function $t \mapsto \operatorname{sgn}(t)|t|^{\alpha-1}$ shows that, for $\alpha \in (0,1)$, this quantity is positive when $y_M < 1$ and negative when $y_M > 1$ (and conversely for $\alpha < 0$).

Finally, we treat the case $\alpha > 1$. Using the expression (3.1), in order to prove that $\frac{\partial F_\alpha}{\partial y}(M) > 0$, we prove that $g : u \to u\left(x_M^2 + u^2\right)^{\alpha/2-1}$ is increasing for any $x_M \geq 0$. For $x_M = 0$ the previous argument applies. For $x_M > 0$, g is differentiable and, for $u \in \mathbb{R}$, $g'(u) = [x_M^2 + (\alpha-1)u^2]\left(x_M^2 + u^2\right)^{\alpha/2-2} > 0$. Hence, g is increasing and the result follows. □

The study of function F_α allows one to prove that the curve $C(\alpha, \lambda)$ is obtained from the graph of a real function:

Corollary 3.10. *Let $\alpha \in \mathbb{R} \setminus \{0, 1, 2\}$ and $\lambda \in \mathbb{R}^*$. We assume that $\alpha\lambda > 0$, which ensures that the curve $C(\alpha, \lambda)$ is in the upper half-plane.*

For $\alpha < 1$, the curve $C(\alpha, \lambda)$ is bounded. If the curve is nonempty, there exists $0 < y_- < 1 < y_+$ such that $C(\alpha, \lambda) \cap (AB) = \{(0, y_-), (0, y_+)\}$. For any $y \in [y_-, y_+]$, there exists a unique $g_\alpha(y) \geq 0$ such that $(g_\alpha(y), y) \in C(\alpha, \lambda)$. The function g_α is C^1 on (y_-, y_+).

For $\alpha > 1$, the curve $C(\alpha, \lambda)$ is unbounded and, for any $x \in \mathbb{R}$, there exists a unique $f_\alpha(x) \in \mathbb{R}$ such that $(x, f_\alpha(x)) \in C(\alpha, \lambda)$. The function f_α is C^1 on $\mathbb{R}$. Moreover, for all $x \in \mathbb{R}$, $f_\alpha(x) > 0$, and on the interval $[0, \infty)$, the function f_α is increasing for $1 < \alpha < 2$, decreasing for $\alpha > 2$.

Proof. The (un)boundedness of the curve follows from the limits of Lemma 3.9, while the existence of g_α, f_α follows from the intermediate value theorem. In addition, by the implicit function theorem, all these functions are C^1. From the definition of the construction curve, we get that, for any $x \in \mathbb{R}$:

$$\frac{\partial F_\alpha}{\partial x}(x, f_\alpha(x)) + f'_\alpha(x)\frac{\partial F_\alpha}{\partial y}(x, f_\alpha(x)) = 0.$$

By Lemma 3.9, for all $x \in \mathbb{R}$, $\frac{\partial F_\alpha}{\partial x}(x, f_\alpha(x)) > 0$; moreover $\frac{\partial F_\alpha}{\partial y}(x, f_\alpha(x)) > 0$ if $\alpha > 2$ and $\frac{\partial F_\alpha}{\partial y}(x, f_\alpha(x)) < 0$ if $1 < \alpha < 2$. The result follows. □

Corollary 3.11. *$C(\alpha, \lambda)$ is a connected curve.*

Proof. By Lemma 3.9, for any $(x, y) \in \mathbb{R}^2$, $\frac{\partial F}{\partial y}(x, y) > 0$. We can therefore use the implicit function theorem along with Corollary 3.10 to get the result. □

We now investigate the asymptotic behaviour of the function f_α at $+\infty$ (and thus the asymptotic direction of the associated construction curve). The following states that in the case $1 < \alpha < 2$, the construction curve admits the perpendicular bisector of $[AB]$ as asymptotic direction, and in the case $\alpha > 2$, it is the actual asymptote of the curve.

Lemma 3.12. *Let $\alpha \in (1, \infty) \setminus \{2\}$, and $\lambda \neq 0$. As $|x| \to \infty$, $f_\alpha(x)$ has the following asymptotic behaviour :*

$$f_\alpha(x) \sim \frac{\lambda}{2\alpha}|x|^{2-\alpha}.$$

Proof. By the symmetry properties of $C(\alpha, \lambda)$, we only have to focus on the case $x \to +\infty$. For any $x > 0$, by the mean value theorem, there exists an $u_x \in (f_\alpha(x) - 1, f_\alpha(x) + 1)$ such that

$$\begin{aligned}
\lambda &= \left(x^2 + (f_\alpha(x) + 1)^2\right)^{\alpha/2} - \left(x^2 + (f_\alpha(x) - 1)^2\right)^{\alpha/2} \\
&= 2\alpha u_x (x^2 + u_x^2)^{\alpha/2-1} \\
&= 2\alpha u_x^{\alpha-1} \left(\frac{u_x}{x}\right)^{2-\alpha} \left(1 + \left(\frac{u_x}{x}\right)^2\right)^{\alpha/2-1}
\end{aligned}$$

For $1 < \alpha < 2$, this implies that $\frac{u_x}{x}$ is bounded, otherwise the right-hand term would diverge towards $+\infty$. From this observation, we get that

$u_x^{\alpha-1}\left(\frac{u_x}{x}\right)^{2-\alpha} = O(1)$ and therefore that $u_x \sim \frac{\lambda}{2\alpha}x^{2-\alpha}$. Since $u_x \in (f_\alpha(x) - 1, f_\alpha(x) + 1)$, the same holds for $f_\alpha(x)$.

For $\alpha > 2$, as $x \to \infty$, u_x has to converge to 0, and therefore $f_\alpha(x)$ is bounded. Asymptotically, as $x \to \infty$,

$$\begin{aligned}\lambda &= \left(x^2 + (f_\alpha(x)+1)^2\right)^{\alpha/2} - \left(x^2 + (f_\alpha(x)-1)^2\right)^{\alpha/2} \\ &\sim \frac{\alpha}{2}x^{\alpha-2}\left[(f_\alpha(x)+1)^2 - (f_\alpha(x)-1)^2\right] \\ &\sim 2\alpha f_\alpha(x)x^{\alpha-2}.\end{aligned}$$

□

3.4 Flip property for $\alpha > 1$

We now go back to the study of the flip property of α-realizations. we get the following result in the case $\alpha > 1$:

Theorem 3.13. *For $\alpha > 1$, the set of α-realizations satisfies the flip property.*

Proof. Fix $\alpha > 1$ and consider six distinct points $A_1, \dots, A_6$, no three of them being aligned. Suppose that there is a point A_0 such that the quadrilaterals $A_1A_2A_3A_0$, $A_3A_4A_5A_0$ and $A_5A_6A_1A_0$ are all α-quads. Then, by combining the equations of these α-quads, we get

$$A_1A_2^\alpha - A_2A_3^\alpha + A_3A_4^\alpha - A_4A_5^\alpha + A_5A_6^\alpha - A_6A_1^\alpha = 0 \tag{3.2}$$

Consider the following two construction curves: $\mathcal{C}_1$ with foci A_2, A_6 going through A_1, and $\mathcal{C}_3$ with foci A_2, A_4 going through A_3. By Lemma 3.12, $\mathcal{C}_1$ admits $P(A_2A_6)$ as an asymptotic direction, and $\mathcal{C}_3$ admits $P(A_2A_4)$ as an asymptotic direction. These two lines are not parallel, since A_2, A_4, A_6 are not aligned. Therefore, considering the behaviour of $\mathcal{C}_1$ and $\mathcal{C}_3$ at infinity and using Corollary 3.11, these two construction curves have to intersect an odd number of times, and thus at least once. Let us therefore denote by A_7 a point of intersection of the curves.

By definition of the two construction curves, we have

$$\begin{aligned}A_6A_1^\alpha - A_1A_2^\alpha + A_2A_7^\alpha - A_7A_6^\alpha = 0,\\ A_2A_3^\alpha - A_3A_4^\alpha + A_4A_7^\alpha - A_7A_2^\alpha = 0.\end{aligned}$$

Summing these two relations to (3.2), we get

$$A_5A_6^\alpha - A_6A_7^\alpha + A_7A_4^\alpha - A_4A_5^\alpha = 0.$$

Hence, $A_4A_5A_6A_7$ is an α-quad, and $A_1, \dots, A_7$ form indeed an α-realization of the right-hand side of Figure 5. □

Remark 3.14. It may be interesting to bound the number of intersection points of two construction curves having a focus in common, in order to control the number of potential points that could appear. Based on simulations, we expect that for $\alpha < 1$ there are at most two points of intersection, and for $\alpha > 1$ there are at most three (see the examples of Figure 7). It should be possible to use an analysis similar to that of Lemma 3.9 to get properties of convexity of the construction curves and deduce the previous bounds, but we have not succeeded yet.

4 1-embeddings and their cube move

Our goal in this section is to prove the unique proper flip property for 1-embeddings.

Theorem 4.1. *The set of* 1*-embeddings satisfies the unique proper flip property.*

Although our proof only worksin this specific case, we expect the following more general result to hold:

Conjecture 4.2. *For any $\alpha \in [-\infty, 1]$, for any six distinct points in the plane $A_1, A_2, \dots, A_6$, no three of them being aligned, the following are equivalent:*

- *there exists a* unique *point A_0 such that $A_0, A_1, \dots, A_6$ is an* α-embedding *of the graph on the left-hand side of Figure 5;*
- *there exists a* unique *point A_7 such that $A_1, \dots, A_7$ is an* α-embedding *of the graph on the right-hand side of Figure 5.*

Notice that this is weaker than the unique proper flip property, as it is possible that several points A_0 exist and no point A_7. Such a configuration is shown in the top-left picture of Figure 7.

The rest of this section is devoted to the proof of Theorem 4.1.

4.1 Uniqueness

In this first part, we prove the following proposition, which states the uniqueness of the point A_0, if it exists.

Proposition 4.3. *For any proper, positively oriented hexagon $A_1, A_2, \dots, A_6$, there exists at most one point A_0 such that $A_0, A_1, \dots, A_6$ is a proper* 1*-embedding of the left-hand side of Figure 5.*

In order to prove it, we first need some information on the geometric properties of 1-quads. Notice that if three distinct point A, B, C are fixed, then the construction curve for 1-quads is the set of points D such that

$$AD - CD = AB - BC.$$

Hence, it is a hyperbola branch with foci A, C (with possible degenerate cases being the perpendicular bisector of $[AC]$, and half-lines $A + t(A - C)$ or $C + t(C - A)$ for $t \geq 0$). We put all these cases under the same name:

Definition 4.4. Let A, C be two distinct points in the plane. For any $\lambda \in \mathbb{R}$, the set of points D in the plane such that

$$AD - CD = \lambda \tag{4.1}$$

is called a *generalised hyperbola branch* with foci A and C.

The following lemma already implies that there are at most two admissible points A_0, in the sense of Proposition 4.3.

Lemma 4.5. *Assume that two generalised hyperbola branches have exactly one common focus, then they have at most two intersection points.*

Although this result, which appears in [20, 24], has a very classical flavor, we could not find any earlier reference. We give an alternative proof below.

Proof of Lemma 4.5. If one of the generalised branches is a line or a half-line, the result easily comes from the fact that a hyperbola and a line have at most two points of intersection; we now suppose that it is not the case.

Let us start with some definitions. The focus of a hyperbola branch $\mathcal{B}$ which belongs to (resp. does not belong to) the convex hull of $\mathcal{B}$ is said to be the *interior* (resp. *exterior*) focus of $\mathcal{B}$. For example, on Figure 8, A_1 is the interior focus of both branches while A_3 and A_5 are the exterior foci of these branches. Assume that $\mathcal{B}_1$ is a hyperbola branch with foci A and C and $\mathcal{B}_2$ is a hyperbola branch with foci A and E, with A, C, E distinct. Then any intersection point of $\mathcal{B}_1$ and $\mathcal{B}_2$ lies on a hyperbola branch $\mathcal{B}_3$ with foci C and E (this can be seen by subtracting the equations (4.1) for $\mathcal{B}_1$ and $\mathcal{B}_2$), and we can also suppose that $\mathcal{B}_3$ is not a line or a half-line. Then there is at least one of the three points A, C or E which is the interior focus of one branch and the exterior focus of another branch. Without loss of generality, we assume that A is the interior focus of $\mathcal{B}_1$ and the exterior focus of $\mathcal{B}_2$. We will show that these two branches intersect in at most two points.

Suppose that $\mathcal{B}_1$ and $\mathcal{B}_2$ intersect at three distinct points S, T, U. As these points belong to a non-degenerate hyperbola branch, they are not aligned. The lines $(ST), (TU), (SU)$ therefore delimit exactly seven open regions in the plane, three of which touching the triangle STU only at one vertex. We call these three regions the *corner chambers* of S, T, U.

Lemma 4.6. *Let S, T and U be three distinct points on a hyperbola branch $\mathcal{B}$. Then the exterior focus of $\mathcal{B}$ belongs to a corner chamber of S, T, U, and the interior focus does not.*

Before proving it, notice that this result is enough to conclude the proof of Lemma 4.5, as A should be both in a corner chamber of S, T, U (because A is the exterior focus of $\mathcal{B}_2$) and not in one (because A is the interior focus of $\mathcal{B}_1$). □

Proof of Lemma 4.6. For any two distinct points A, B on $\mathcal{B}$, the line (AB) cuts the interior of the convex hull of $\mathcal{B}$ into a finite part and an infinite part. The half-plane delimited by (AB) that contains the finite part is called the *exterior half-plane* of A, B. It is easy to see that the exterior focus belongs to the exterior half-plane of A, B, for instance by noting that this property is invariant by affine transformations of the plane, and is straightforward to prove for the special branch $\{(x, y) \in (0, \infty)^2 \mid xy = 1\}$.

Suppose that T belongs to the exterior half-plane of S, U (which is equivalent to saying that S, T, U are met in that order when following the branch $\mathcal{B}$). Then, applying the previous property to (S, T) and (T, U), we get that the exterior focus has to belong to the corner chamber that touches T.

Let us now look at the interior focus of $\mathcal{B}$. By convexity of $\mathcal{B}$, the corner chambers are disjoint from the interior of the convex hull of $\mathcal{B}$, which by definition contains its interior focus. The result follows. □

We can now prove Proposition 4.3.

Proof of Proposition 4.3. Suppose that there exists such a point A_0. As the hexagon is made of three 1-quads, we have by definition

$$A_1A_2 + A_3A_4 + A_5A_6 = A_2A_3 + A_4A_5 + A_6A_1. \tag{4.2}$$

The admissible point A_0 has to be at the intersection of the three generalised hyperbola branches associated to the three 1-quads (those going through A_{i+1} with foci A_i, A_{i+2}, for $i \in \{1, 3, 5\}$, with the convention that $A_7 = A_1$). Notice that $A_1A_2 < A_2A_3$ if and only if A_1 is the interior focus of the hyperbola branch with foci A_1, A_3 going through A_2.

Using this and relation (4.2), we see that one of the points A_1, A_3, A_5 must be the interior focus of both hyperbola branches associated to it (otherwise every term on the left of (4.2) would be smaller than a term on the right, or the converse). Without loss of generality assume that this point is A_1. As A_0 has to be at the intersection of the three branches, by Lemma 4.5 there is at most one other possible point A_0'.

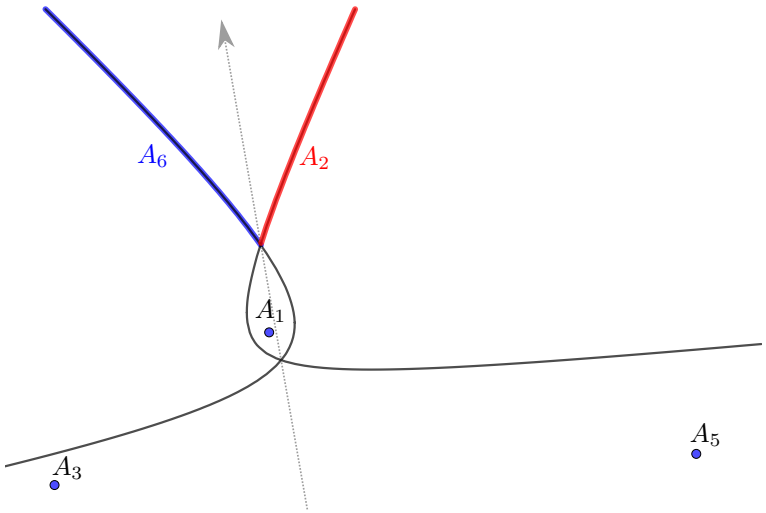

Figure 8: The case of two intersections of the branches. The focus A_1 is the interior focus of both branches.

We now proceed by contradiction, assuming that both A_0 and A_0' provide proper embeddings of the left-hand side of Figure 5. The situation is shown in Figure 8, in the case where the triangle $A_1A_3A_5$ is oriented in that order counterclockwise. For $A_1A_2A_3A_0$ and $A_1A_2A_3A_0'$ to be both proper quadrilaterals oriented as in Figure 5, A_2 has to belong to the red part of the hyperbola. Similarly, A_6 can only belong to the blue part of the second hyperbola. For the rest of the proof we assign Cartesian coordinates to the points in the plane, with the x axis parallel to (A_0A_0') and directed from A_0 to A_0'. Take a point A_2 on the red part, and draw the segment $[A_2A_3]$. By the assumption that the embedding is proper, this segment cannot intersect $[A_1A_6]$. Hence $x_{A_6} < x_{A_2}$. Arguing similarly on the segments $[A_5A_6]$ and $[A_1A_2]$, we get that $x_{A_2} < x_{A_6}$, which yields the desired contradiction.

The case where the triangle $A_1A_3A_5$ is oriented in that order clockwise is almost identical, with the only difference that one has to consider the intersection of $[A_2A_3]$ and $[A_5A_6]$ to conclude. □

4.2 Existence

The second part of this section consists in proving that, if we start with a proper 1-embedding $A_0, A_1, \ldots, A_6$ of the left-hand side of Figure 5, then there actually exists a point A_7 inducing a proper 1-embedding of the right-hand side. To show this, we transform the problem into a linear one by using the *propagation equations* and *s-embeddings* defined by Chelkak [5]. We first explain this construction, then give a few extra properties concerning the ordering of the vertices of the quads it gives, and finally apply it to our setting.

4.2.1 Ising model, propagation equations and s-embeddings

Let $G := (V, E)$ be a finite planar graph, in which each edge $e \in E$ carries a positive weight $J_e > 0$. The weights $(J_e)_{e\in E}$ are called the coupling constants of the ferromagnetic Ising model on G, that is, every spin configuration $\sigma \in \{\pm 1\}^V$ is assigned the Boltzmann weight

$$w(\sigma) = \exp\left(\sum_{e=\{u,v\}\in E} J_e\sigma_u\sigma_v\right)$$

and a spin configuration is randomly sampled with probability proportional to its Boltzmann weight. Note however that we will not refer to any statistical mechanical property of the Ising model thereafter; all the proofs are of purely geometric nature.

For every $e \in E$ there exists a unique $\theta_e \in (0, \frac{\pi}{2})$ such that

$$J_e = \frac{1}{2}\ln\left(\frac{1+\sin\theta_e}{\cos\theta_e}\right). \tag{4.3}$$

We also set

$$x_e = \tanh J_e = \tan\frac{\theta_e}{2} \in (0, 1). \tag{4.4}$$

Let G^c be the graph whose vertices are the *corners* of the faces of G, and whose edges are of two types:

1. those connecting two corners that correspond to the same vertex and to the same edge e of G; such edges carry the weight $\cos\theta_e$;
2. those connecting two corners that correspond to the same face and to the same edge e of G; such edges carry the weight $\sin\theta_e$.

See Figure 9 for an illustration. There exists a double cover $\Upsilon^\times$ of G^c that branches around every edge, vertex and face of G, graphically represented around an edge in Figure 10 (see also Figure 15). It inherits the edge weights of G^c.

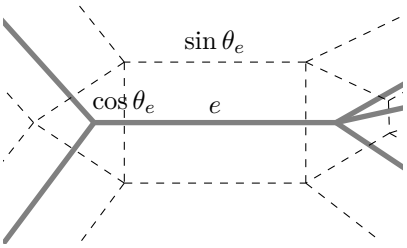

Figure 9: The corner graph G^c (dashed) around an edge e of G (solid).

Let $V^\times$ be the vertices of $\Upsilon^\times$. We say that a function $X : V^\times \to \mathbb{C}$ satisfies the *propagation equation* if, for every $v \in V^\times$ with neighbours $v', v'' \in V^\times$ around an edge e like in Figure 10,

$$X_v = \sin\theta_e X_{v'} + \cos\theta_e X_{v''}.$$

It is easy to check that if X satisfies the propagation equation, its value is multiplied by -1 whenever we change sheets above a vertex of G^c.

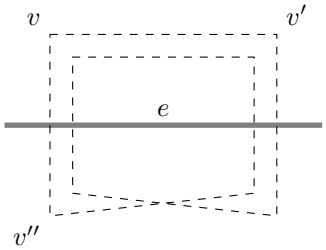

Figure 10: The double cover $\Upsilon^\times$ around the edge e of G.

If X is a solution to the propagation equations, then one can construct a *s-embedding* $\mathcal{S} : G^\diamond \to \mathbb{C}$ the following way.

Fix the image $\mathcal{S}(u_0)$ of a base vertex u_0 of G in the plane. Then define $\mathcal{S}$ such that for every vertex u of G and every face f adjacent to it, denoting by c the corner between u and f,

$$\mathcal{S}(f) - \mathcal{S}(u) = X_c^2$$

where X_c is any of the two values of X above the corner c. See Figure 12 for an example. We will rely on the following result of Chelkak [5] identifying s-embeddings to our notion of 1-embeddings.

Proposition 4.7 ([5])**.** *For any solution X of the propagation equation such that $\mathrm{Re}(X), \mathrm{Im}(X)$ are two vectors independent over $\mathbb{R}$, the associated s-embedding is well-defined, and is such that every face of $G^\diamond$ is sent to a proper 1-quad in the complex plane. Conversely, for any 1-embedding $\mathcal{T}$ of G, for any edge $e \in E$ let θ_e be the unique angle in $\left(0, \frac{\pi}{2}\right)$ such that, using the notation of Figure 11,*

$$\tan^2\theta_e = \frac{\operatorname{cotan}\delta + \operatorname{cotan}\beta}{\operatorname{cotan}\alpha + \operatorname{cotan}\gamma}.$$

Then $\mathcal{T}$ is an s-embedding (in the sense of Chelkak) associated to a solution of the propagation equations on G with parameters $(\theta_e)_{e\in E}$.

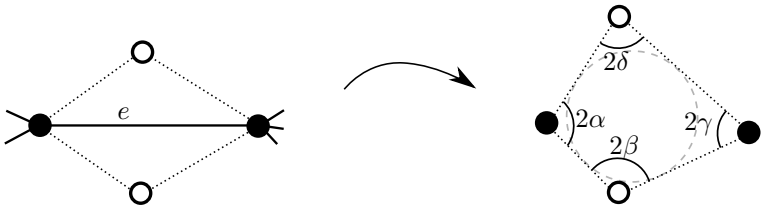

Figure 11: From an abstract graph to a 1-embedding.

The plan of our proof of the existence part of the flip property is therefore to translate the initial configuration into a solution of the propagation equations, then show that one can apply a star-triangle transformation on this solution, and finally to go back to embeddings. However, we need a bit more information than what is contained in Proposition 4.7, as we want to keep track of the orientation of quadrilaterals. This is the aim of the following subsection.

4.2.2 Orientation of quads in s-embeddings

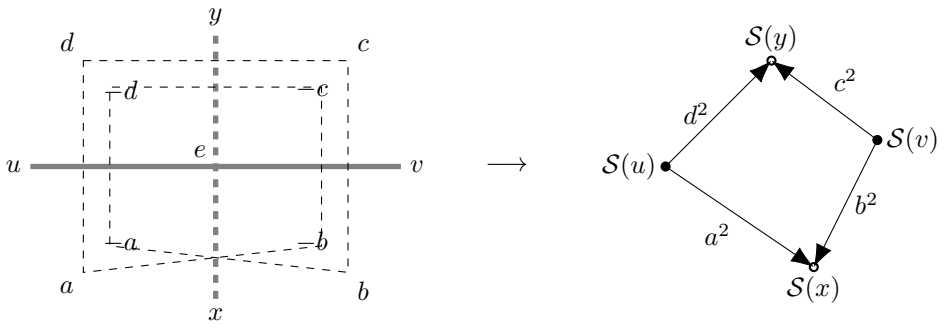

Figure 12: An edge $e \in E$ with vertices u, v and adjacent faces x, y, with a solution of its propagation equation, and the corresponding s-embedding, where the numbers $a^2, \dots, d^2$ are the complex coordinates of the vectors bounding the quad.

Lemma 4.8. *Let $a, b, c, d \in \mathbb{C}^*$ be a solution to the propagation equation at an edge $e \in E$ with parameter $\theta \in \left(0, \frac{\pi}{2}\right)$, set around e as in Figure 12. Suppose that $b/a \notin \mathbb{R}$. Then the following are equivalent:*

(i) The 1-quad $\mathcal{S}(u)\mathcal{S}(x)\mathcal{S}(v)\mathcal{S}(y)$ is positively oriented;

(ii) $\mathrm{Im}(b/a) > 0$*;*

(iii) The arguments of $\pm a, \pm b, \pm c, \pm d$ are in the cyclic order $(a, d, c, b, -a, -d, -c, -b)$ around the circle (as in Figure 13).

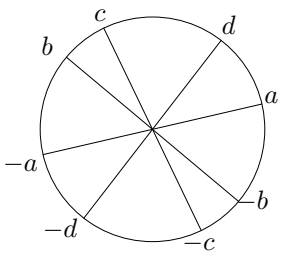

Figure 13: Cyclic order of the arguments of the complex numbers a, b, c, d.

Proof. The three statements are unaltered if we multiply all the complex numbers a, b, c, d by the same nonzero complex number, hence we can suppose $a = 1$. Since the quad $\mathcal{S}(u)\mathcal{S}(x)\mathcal{S}(v)\mathcal{S}(y)$ is proper by Proposition 4.7, the sum of the representatives in $(0, 2\pi)$ of the oriented angles between pairs of vectors $(\widehat{a^2, d^2}), (\widehat{b^2, a^2}), (\widehat{c^2, b^2}), (\widehat{d^2, c^2})$ has to be either 2π if the quad is oriented positively or 6π if the quad is oriented negatively. In particular, the quad is oriented positively (resp. negatively) if and only if the arguments of a^2, d^2, c^2, b^2 (resp. b^2, c^2, d^2, a^2) are in that cyclic order around the circle.

- $(iii) \Rightarrow (i)$: Immediate consequence of the previous sentence.
- $(ii) \Rightarrow (iii)$: Suppose that $\mathrm{Im}(b) > 0$. Solving the propagation equation gives

$$c = \frac{b}{\cos\theta} + \tan\theta,$$
$$d = \frac{1}{\cos\theta} + b\tan\theta.$$

  Thus c and d are positive combinations of 1 and b, so their complex arguments lie between 0 and that of b. Moreover, by a computation,

$$\mathrm{Im}\left(\frac{c}{d}\right) = \frac{\cos^2\theta\,\mathrm{Im}(b)}{|1 + b\sin\theta|^2} > 0$$

  and we deduce that the order of the arguments matches the one of Figure 13.

- $(i) \Rightarrow (ii)$: Assume that (ii) is not verified, that is, $\mathrm{Im}(b) < 0$. Then consider $\bar{b}, \bar{c}, \bar{d}$, which is still a solution to the propagation equation as this equation has real coefficients. But these values do satisfy (ii), hence also (iii) and thus (i) by the previous points. Note that they correspond to a quadrilateral that is the image by a reflection of our desired quad $\mathcal{S}(u)\mathcal{S}(x)\mathcal{S}(v)\mathcal{S}(y)$, and therefore for our initial solution (i) does not hold.

□

4.2.3 Star-triangle transformation on propagation equations

This part consists in rephrasing Baxter's results on the star-triangle transformation of the Ising model; see Section 6.4 of [3]. It is slightly easier to present

it in the triangle-star direction, *i.e.* from the right-hand side to the left-hand side of Figure 14, although the converse is also possible.

Let us suppose that the graph G contains a triangle, as on the right-hand side of Figure 14. We label its edges with the parameters θ_i, and we define as well x_i, J_i as in (4.3) and (4.4). It is possible to transform the triangle into the star displayed on the left-hand side, while finding parameters such that both Ising models are coupled and agree everywhere except at A_7. This is called the *star-triangle transformation*.

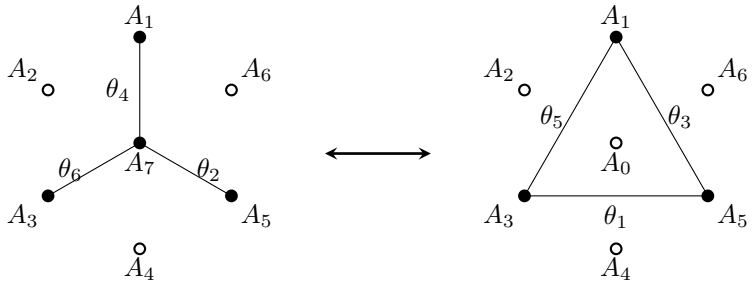

Figure 14: Star-triangle transformation on G (black vertices)

Proposition 4.9 ([3])**.** *Let $k' \in (0, \infty)$ be defined as*

$$k' = \frac{(1-x_1^2)(1-x_3^2)(1-x_5^2)}{4\sqrt{(1+x_1x_3x_5)(x_1+x_3x_5)(x_3+x_1x_5)(x_5+x_1x_3)}}.$$

Then the parameters $\theta_2, \theta_4, \theta_6$ obtained by the star-triangle transformation are the unique angles in $(0, \frac{\pi}{2})$ such that

$$\forall i \in \{1,3,5\},\ \tan\theta_i \tan\theta_{i+3} = \frac{1}{k'} \tag{4.5}$$

where the labels of the angles are considered modulo 6.

Remark 4.10. This transformation may be expressed in different ways. The previous definition of k' naturally comes from the use of an *elliptic modulus* $k \in i\mathbb{R} \cup [0,1)$ such that $k^2 + k'^2 = 1$; see Appendix A for a short introduction to elliptic functions.

We can define elliptic angles $\tau_1, \dots, \tau_6$ and $\theta'_1, \dots, \theta'_6$ by

$$\tau_i = \mathrm{F}(\theta_i, k),$$
$$\theta'_i = \frac{\pi\tau_i}{2\mathrm{K}(k)}.$$

where F (resp. K) is the incomplete (resp. complete) integral of the first kind, see Appendix A for definitions and details. The normalization is such that both θ and θ' variables live in $(0, \frac{\pi}{2})$, while τ variables live in $(0, K(k))$. Then k can be seen as the only modulus such that the θ' angles satisfy

$$\theta'_1 + \theta'_3 + \theta'_5 = \frac{\pi}{2}. \tag{4.6}$$

In these parameters, the star-triangle transformation simply reads

$$\forall i \in \{1,3,5\},\ \theta'_{i+3} = \frac{\pi}{2} - \theta'_i. \tag{4.7}$$

The graphs $\Upsilon^\times$ corresponding to the star and to the triangle configurations are represented in Figure 15. We show that when the angles θ are chosen to satisfy the star-triangle relations (4.5), the propagation equations "seen from the boundary vertices" $x_1, \dots, x_6$ are the same.

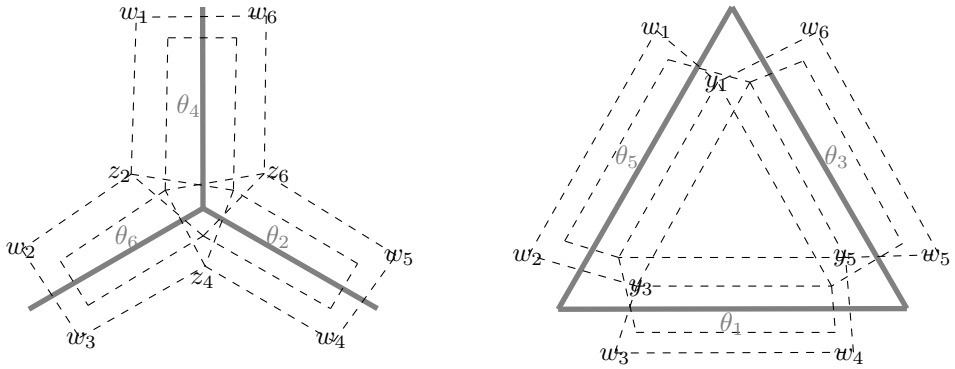

Figure 15: Star-triangle transformation of $\Upsilon^\times$.

Proposition 4.11. *Suppose that $\theta_1, \dots, \theta_6 \in (0, \frac{\pi}{2})$ satisfy the star-triangle relations (4.5). Let $(w_1, w_2, w_3, w_4, w_5, w_6, y_1, y_3, y_5)$ be a solution of the propagation equations on the "triangle" graph on the right of Figure 15. Then there exists a unique triple (z_2, z_4, z_6) such that $(w_1, w_2, w_3, w_4, w_5, w_6, z_2, z_4, z_6)$ is a solution of the propagation equations on the "star" graph on the left. Conversely, for any solution $(w_1, w_2, w_3, w_4, w_5, w_6, z_2, z_4, z_6)$ on the left, there exists a unique triple y_1, y_3, y_5 such that $(w_1, w_2, w_3, w_4, w_5, w_6, y_1, y_3, y_5)$ is a solution on the right.*

Proof. It is easy to see that any values of (y_1, y_3, y_5) uniquely characterize the solution of the propagation equations on the triangle graph. Thus the set of possible vectors $(w_1, \dots, w_6)$ is a 3-dimensional subspace V. By setting (y_1, y_3, y_5) to be the elements of the canonical basis of $\mathbb{C}^3$ and solving the propagation equations, we get a basis of V:

$$u_1 = \begin{pmatrix} 1/\cos\theta_5 \\ \tan\theta_5 \\ 0 \\ 0 \\ \tan\theta_3 \\ 1/\cos\theta_3 \end{pmatrix}, u_3 = \begin{pmatrix} \tan\theta_5 \\ 1/\cos\theta_5 \\ 1/\cos\theta_1 \\ \tan\theta_1 \\ 0 \\ 0 \end{pmatrix}, u_5 = \begin{pmatrix} 0 \\ 0 \\ \tan\theta_1 \\ 1/\cos\theta_1 \\ 1/\cos\theta_3 \\ \tan\theta_3 \end{pmatrix}.$$

Similarly, the set of values of $(w_1, \dots, w_6)$ for the star graph is a subspace V' with basis

$$v_2 = \begin{pmatrix} 1/\sin\theta_4 \\ 1/\sin\theta_6 \\ 1/\tan\theta_6 \\ 0 \\ 0 \\ 1/\tan\theta_4 \end{pmatrix}, v_4 = \begin{pmatrix} 0 \\ 1/\tan\theta_6 \\ 1/\sin\theta_6 \\ 1/\sin\theta_2 \\ 1/\tan\theta_2 \\ 0 \end{pmatrix}, v_6 = \begin{pmatrix} 1/\tan\theta_4 \\ 0 \\ 0 \\ 1/\tan\theta_2 \\ 1/\sin\theta_2 \\ 1/\sin\theta_4 \end{pmatrix}.$$

We want to show that these subspaces are equal. By an argument of dimension, we just need to show that $v_2, v_4, v_6 \in V$. Let us do it for v_2, the other cases being symmetric. We claim that

$$\frac{1}{\cos\theta_3 \tan\theta_4} u_1 + \frac{1}{\cos\theta_1 \tan\theta_6} u_3 - \frac{\tan\theta_1}{\tan\theta_6} u_5 = v_2.$$

This is checked immediately for the third and fourth entries; the fifth and sixth entries are similar after noting that by (4.5),

$$\frac{\tan\theta_1}{\tan\theta_6} = \frac{\tan\theta_3}{\tan\theta_4}. \tag{4.8}$$

The first and second entries are a bit more tedious. For the first one, we want to show that

$$\frac{1}{\cos\theta_3 \tan\theta_4 \cos\theta_5} + \frac{\tan\theta_5}{\cos\theta_1 \tan\theta_6} = \frac{1}{\sin\theta_4}. \tag{4.9}$$

In terms of the elliptic variables $\tau_i = F(\theta_i, k)$ (see Appendix A), this amounts to showing (we omit the elliptic parameter k):

$$\mathrm{nc}(\tau_3)\,\mathrm{cs}(\tau_4)\,\mathrm{nc}(\tau_5) + \mathrm{nc}(\tau_1)\,\mathrm{sc}(\tau_5)\,\mathrm{cs}(\tau_6) - \mathrm{ns}(\tau_4) = 0. \tag{4.10}$$

By (4.7), $\tau_4 = \mathrm{K}(k) - \tau_1$ and $\tau_6 = \mathrm{K}(k) - \tau_3$, and by (4.6), $\tau_1 = \mathrm{K}(k) - (\tau_3 + \tau_5)$. Thus we can express all the arguments in terms of τ_3, τ_5. Using the change of arguments in elliptic functions (A.1), the left-hand side of (4.10) is equal to

$$\begin{aligned}
&\mathrm{nc}(\tau_3)\,\mathrm{nc}(\tau_5)\,\mathrm{cs}(\tau_3+\tau_5) + \mathrm{sc}(\tau_3)\,\mathrm{sc}(\tau_5)\,\mathrm{ds}(\tau_3+\tau_5) - \mathrm{ns}(\tau_3+\tau_5) \\
&= \mathrm{nc}(\tau_3)\,\mathrm{nc}(\tau_5)\,\mathrm{ns}(\tau_3+\tau_5)\times \\
&\qquad \left(\mathrm{cn}(\tau_3+\tau_5) + \mathrm{sn}(\tau_3)\,\mathrm{sn}(\tau_5)\,\mathrm{dn}(\tau_3+\tau_5) - \mathrm{cn}(\tau_3)\,\mathrm{cn}(\tau_5)\right).
\end{aligned}$$

By (A.2), this is equal to zero.

For the second entry, we want to show that

$$\frac{\tan\theta_5}{\cos\theta_3 \tan\theta_4} + \frac{1}{\cos\theta_1 \tan\theta_6 \cos\theta_5} = \frac{1}{\sin\theta_6}. \tag{4.11}$$

By (4.5), $\frac{\tan\theta_5}{\tan\theta_4} = \frac{\tan\theta_1}{\tan\theta_2}$. Hence (4.11) is equivalent to

$$\frac{\tan\theta_1}{\cos\theta_3 \tan\theta_2} + \frac{1}{\cos\theta_1 \tan\theta_6 \cos\theta_5} = \frac{1}{\sin\theta_6}.$$

Up to a cyclic shift, this is the same as (4.9), so it holds by the previous discussion. □

As a byproduct of the previous proof, we obtain Theorem 1.2, formulas expressing the change of θ parameters in the star-triangle transformation. These formulas are much simpler than the classical computation described in Proposition 4.9 and to the best of our knowledge, they are new.

Proof of Theorem 1.2. For $i = 4$, this follows from combining equations (4.8) and (4.9). Cyclic shifts of indices give the cases $i = 2$ and $i = 6$.

To obtain the other three values of i, we apply the Kramers-Wannier duality of the Ising model [17], which has the effect of transforming the variables θ_i into $\frac{\pi}{2} - \theta_i$. In this duality, the star graph becomes its dual, *i.e.* a triangle, and vice-versa. Hence the formula can be deduced from the previous one by changing sines into cosines and vice-versa. □

We now have all the elements to prove the unique proper flip property of 1-embeddings.

Proof of Theorem 4.1. We start with $A_0, A_1, \dots, A_6$ a proper embedding of the left-hand side of Figure 5. As uniqueness is a consequence of Proposition 4.3, we just have to prove that there exists a point A_7 such that $A_1, A_2, \dots, A_7$ is a proper embedding of the right-hand side.

By Proposition 4.7, there exists $(w_1, w_2, w_3, w_4, w_5, w_6, y_1, y_3, y_5)$ a solution of the propagation equation as on the left-hand side of Figure 15 such that the initial points $A_0, A_1, \dots, A_6$ are the s-embedding of this solution. Hence by Proposition 4.11, there exists (z_2, z_4, z_6) such that $(w_1, w_2, w_3, w_4, w_5, w_6, z_2, z_4, z_6)$ is a solution to the propagation equations of the right-hand side of Figure 15. Let us consider its s-embedding. It has the same boundary as the initial one, hence the points $A_1, \dots, A_6$ are unchanged, and we have a new point A_7. It remains to prove that the three new 1-quads are proper and oriented as on the right-hand side of Figure 5. As no three vertices of the hexagon are aligned, x_1/x_2 is not a real number; moreover the initial quad $A_1A_2A_3A_0$ is proper and positively oriented. Hence we can apply Lemma 4.8 to obtain the ordering of the arguments of x_1, x_2, y_3, y_1. By doing the same for the other two initial quads, the order of the arguments of the variables x_i and y_i is that on the left of Figure 16.

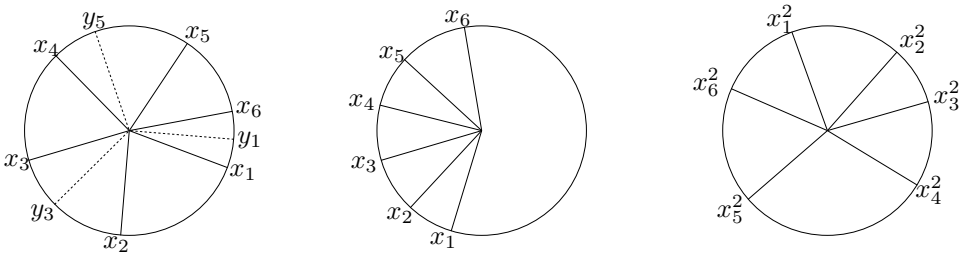

Figure 16: The cyclic order of the arguments of the variables x_i and y_i.

Let us prove that the new (proper) quad $A_1A_2A_7A_6$ is positively oriented. By Lemma 4.8, it is enough to prove that $\mathrm{Im}(x_6/x_1) > 0$. If this is not the case, then we are in the situation of the second configuration of Figure 16, where all the arguments are included in a half-circle. Therefore we can get the order of the arguments of the x_i^2, as in the picture on the right of Figure 16. However, as in the proof of Lemma 4.8, the successive internal angles of the hexagon $A_1A_2A_3A_4A_5A_6$ can be expressed as the successive oriented angles in direct order in this last figure, hence their sum is 2π. This contradicts the fact that the hexagon is non-crossed, as the sum should be 4π. By symmetry, the three new quads are properly oriented, which concludes the proof. □

Remark 4.12. The so-called *exact bosonization* operation provides a map from an Ising model on some planar graph G to a bipartite dimer model on a modified graph $\widetilde{G}$ [6]. Under this correspondence, the Ising star-triangle move corresponds to the composition of six local moves for the dimer model called urban renewals ([15], Fig. 6). On the other hand, embeddings as centers of circle patterns are known to be adapted to bipartite dimer models and the counterpart of urban renewal for these geometric objects is called the Miquel move [13].

From all this we conclude that it is possible to write the star-triangle move for s-embeddings as a composition of six Miquel moves.

5 f-quadrilaterals

This last short section proposes a generalization of our notion of α-quads, where one replaces the function $f_\alpha : (x, y) \mapsto x^\alpha + y^\alpha$ by any function of the following form; it appears that some results still hold in this broader framework.

Definition 5.1. Let $f : (\mathbb{R}_+)^2 \to \mathbb{R}$ be a symmetric function of two variables. The function f is said to be *homogeneous* if there exists $u \in \mathbb{R}$ such that for any $\lambda, x, y > 0$, we have $f(\lambda x, \lambda y) = \lambda^u f(x, y)$.

Definition 5.2. Let $f : (\mathbb{R}_+)^2 \to \mathbb{R}$ be a non-constant homogeneous symmetric function of two variables. A quadrilateral $ABCD$ is called an *f-quadrilateral* if

$$f(AB, CD) = f(BC, AD).$$

Multiplying f by a non-zero scalar, or more generally post-composing it with a bijection, produces the same class of quads. The α-quads arise as f_α-quadrilaterals.

A variant of Proposition 2.6 characterizing α-quads via circumradii of the triangles formed by the vertices and the intersection point of the diagonals also holds for f-quadrilaterals.

Proposition 5.3. *Let $ABCD$ be a quad with P denoting the intersection point of its diagonals. We denote the circumradii of the triangles ABP, BCP, CDP, DAP by R_1, R_2, R_3, R_4. Let $f : (\mathbb{R}_+)^2 \to \mathbb{R}$ be a symmetric homogeneous function. The following are equivalent:*

1. *$ABCD$ is an f-quadrilateral ;*
2. *$f(R_1, R_3) = f(R_2, R_4)$.*

The proof is identical to the one of Proposition 2.6, as the only property of f_α that is necessary in that proof is its homogeneity.

We end this section with an open question.

Question 5.4. Apart from f_α, are there homogeneous functions f such that f-quadrilaterals satisfy one of the flip properties discussed in this paper?

Acknowledgements

We are grateful to Dmitry Chelkak, Marianna Russkikh and Andrea Sportiello for numerous fruitful discussions. We also thank Thomas Blomme and Othmane Safsafi for discussions leading to the proof of Propositions 2.5 and 2.6. PM and SR are partially supported by the Agence Nationale de la Recherche, Grant Number ANR-18-CE40-0033 (ANR DIMERS). SR also acknowledges the support of the Fondation Sciences Mathématiques de Paris. PT acknowledges partial support from Agence Nationale de la Recherche, Grant Number ANR-14-CE25-0014 (ANR GRAAL).

A Jacobi elliptic functions

In this appendix we give a very brief presentation of elliptic functions and formulas used in the paper, with variable names that are not classical but fit the framework of our paper. For a more complete introduction, we refer to [18, 1].

Consider a number $k \in [0,1) \cup i\mathbb{R}$, which we call *elliptic modulus*. Let $k' = \sqrt{1-k^2}$. We first define the *incomplete integral of the first kind*:

$$F(\theta, k) = \int_0^\theta \frac{dt}{\sqrt{1 - k^2 \sin^2 t}}.$$

The function $F(\cdot, k)$ is a bijection from $\mathbb{R}$ to $\mathbb{R}$, and we denote its inverse by $\mathrm{am}(\cdot, k)$. Then the two first Jacobi elliptic functions are defined for any $\tau \in \mathbb{R}$ by

$$\begin{aligned} \mathrm{cn}(\tau, k) &= \cos(\mathrm{am}(\tau, k)), \\ \mathrm{sn}(\tau, k) &= \sin(\mathrm{am}(\tau, k)). \end{aligned}$$

These functions can be thought of as generalizations of usual cosine and sine functions. For $k = 0$, the function $F(\cdot, k)$ is clearly the identity, hence cn and sn reduce to cos and sin. In general, they are periodic functions, of period $4K(k)$ where K denotes the *complete integral of the first kind*, also named *quarter-period*:

$$K(k) = F\left(\frac{\pi}{2}, k\right).$$

Apart from cn and sn, we also define

$$\mathrm{dn}(\tau, k) = \sqrt{1 - k^2 \,\mathrm{sn}(\tau, k)}.$$

Then, for any two distinct letters $p, q \in \{c, s, d, n\}$, we define a function pq as $\frac{pn}{qn}$, with the convention that $nn = 1$. For instance,

$$\begin{aligned} \mathrm{nc}(\tau, k) &= \frac{1}{\mathrm{cn}(\tau, k)}, \\ \mathrm{sc}(\tau, k) &= \frac{\mathrm{sn}(\tau, k)}{\mathrm{cn}(\tau, k)}, \end{aligned}$$

etc.

The following formulas describe how these elliptic functions are affected by the change of variable $\tau \mapsto K(k) - \tau$; they can be found in [1], chapter 16.8. As is customary, we omit the dependence in k to simplify notations.

$$\begin{aligned} \mathrm{cn}(K - \tau) &= k' \,\mathrm{sd}(\tau), \\ \mathrm{sn}(K - \tau) &= \mathrm{cd}(\tau), \\ \mathrm{dn}(K - \tau) &= k' \,\mathrm{nd}(\tau). \end{aligned} \tag{A.1}$$

The effect of the same change of variable on any other function pq can be deduced from these three.

We also make use of an addition identity, that can be found as formula 32(i) in Chapter 2 of [18]. For any $\tau, \tau' \in \mathbb{R}$,

$$\mathrm{cn}(\tau + \tau') + \mathrm{sn}(\tau)\,\mathrm{sn}(\tau')\,\mathrm{dn}(\tau + \tau') - \mathrm{cn}(\tau)\,\mathrm{cn}(\tau') = 0. \tag{A.2}$$

References

[1] Milton Abramowitz and Irene A. Stegun. *Handbook of Mathematical Functions with Formulas, Graphs, and Mathematical Tables*. Dover, New York, ninth Dover printing, tenth GPO printing edition, 1964.

[2] Eisso J. Atzema. A theorem by Giusto Bellavitis on a class of quadrilaterals. *Forum Geom.*, 6:181–185, 2006.

[3] Rodney J. Baxter. *Exactly solved models in statistical mechanics*. Academic Press, London, 1982.

[4] Noam Berger and Marek Biskup. Quenched invariance principle for simple random walk on percolation clusters. *Probab. Theory Related Fields*, 137(1-2):83–120, 2007.

[5] Dmitry Chelkak. Planar Ising model at criticality: state-of-the-art and perspectives. In *Proceedings of the International Congress of Mathematicians—Rio de Janeiro 2018. Vol. IV. Invited lectures*, pages 2801–2828. World Sci. Publ., Hackensack, NJ, 2018.

[6] Julien Dubédat. Exact bosonization of the Ising model. *arXiv preprint*, 2011. arXiv:1112.4399.

[7] Hugo Duminil-Copin, Jhih-Huang Li, and Ioan Manolescu. Universality for the random-cluster model on isoradial graphs. *Electron. J. Probab.*, 23:70 pp., 2018.

[8] Martin Josefsson. When is a tangential quadrilateral a kite? *Forum Geom.*, 11, 2011.

[9] Martin Josefsson. Characterizations of orthodiagonal quadrilaterals. *Forum Geom.*, 12:13–25, 2012.

[10] Shizuo Kakutani. Markoff process and the Dirichlet problem. *Proc. Japan Acad.*, 21:227–233 (1949), 1945.

[11] A. E. Kennelly. Equivalence of triangles and star in conducting networks. *Electrical World and Engineer*, 34:413–414, 1899.

[12] Richard Kenyon. An introduction to the dimer model. In *School and Conference on Probability Theory*, ICTP Lect. Notes, XVII, pages 267–304. Abdus Salam Int. Cent. Theoret. Phys., Trieste, 2004.

[13] Richard Kenyon, Wai Yeung Lam, Sanjay Ramassamy, and Marianna Russkikh. Dimers and Circle patterns. *arXiv preprint*, 2018. arXiv:1810.05616.

[14] Richard Kenyon and Robin Pemantle. Principal minors and rhombus tilings. *Journal of Physics A: Mathematical and Theoretical*, 47(47):474010, nov 2014.

[15] Richard Kenyon and Robin Pemantle. Double-dimers, the Ising model and the hexahedron recurrence. *J. Combin. Theory Ser. A*, 137:27–63, 2016.

[16] B. G. Konopelchenko and W. K. Schief. Reciprocal figures, graphical statics, and inversive geometry of the Schwarzian BKP hierarchy. *Stud. Appl. Math.*, 109(2):89–124, 2002.

[17] H. A. Kramers and G. H. Wannier. Statistics of the Two-Dimensional Ferromagnet. Part I. *Physical Review*, 60:252–262, August 1941.

[18] Derek F. Lawden. *Elliptic Functions and Applications*. Applied Mathematical Sciences. Springer New York, 1989.

[19] Marcin Lis. Circle patterns and critical Ising models. *Comm. Math. Phys.*, 370(2):507–530, 2019.

[20] Dennis Lucarelli, Anshu Saksena, Ryan Farrell, and I-Jeng Wang. Distributed inference for network localization using radio interferometric ranging. *Wireless Sensor Networks*, pages 52–73, 2008.

[21] Lars Onsager. Crystal statistics. I. A two-dimensional model with an order-disorder transition. *Phys. Rev. (2)*, 65:117–149, 1944.

[22] W. T. Tutte. How to draw a graph. *Proc. London Math. Soc. (3)*, 13:743–767, 1963.

[23] Gregory H Wannier. The statistical problem in cooperative phenomena. *Reviews of Modern Physics*, 17(1):50, 1945.

[24] Xiaochun Xu, Sartaj Sahni, and Nageswara S. V. Rao. On basic properties of localization using distance-difference measurements. In *2008 11th International Conference on Information Fusion*, pages 1–8, 2008.

Département de Mathématiques, Université de Fribourg, PER 12 bu. 0.106, Ch. du Musée 11, 1700 Fribourg, Suisse
E-mail address: paul.melotti at unifr.ch

Université Paris-Saclay, CNRS, CEA, Institut de physique théorique, 91191 Gif-sur-Yvette, France
E-mail address: sanjay.ramassamy at ipht.fr

Centre de Mathématiques Appliquées, École polytechnique, Route de Saclay, 91128 Palaiseau Cedex, France
E-mail address: paul.thevenin at polytechnique.edu